Design of Functional Chiral Cyclen-based Radiometal Chelators for Theranostics

Lixiong Dai,[†‡] Junhui Zhang,[†‡] Carlos Tinlong Wong,[†] Wesley Ting Kwok Chan,[†] Xiaoxi Ling,[§] Carolyn J. Anderson,[¢] and Ga-Lai Law[†*]

[†] Department of Applied Biology and Chemical Technology, State Key Laboratory of Chemical Biology and Drug Discovery, The Hong Kong Polytechnic University, Hung Hom, 999077, Hong Kong SAR, China

[§] Departments of Medicine, University of Pittsburgh, Pittsburgh, Pennsylvania 15261, United States

[¢] Departments of Medicine, Radiology, Pharmacology and Chemical Biology, Chemistry, and Bioengineering, University of Pittsburgh, Pittsburgh, Pennsylvania 15261; Departments of Chemistry and Radiology, University of Missouri, Columbia, MO 65211, United States

Supporting Information Placeholder

ABSTRACT: A series of water-soluble chiral cyclen-based chelators with chemical handles for selective targeting have been synthesized (cyclen = 1,4,7,10-Tetraazacyclododecane). Optical studies, relaxivity measurements, and competitive titrations were performed to show the versatility of these chiral chelators. The complexations of L3, L4 and L5 with Lu^{3+}, Y^{3+}, Sc^{3+} and Cu^{2+} were successfully demonstrated in around 90% to 100% yields. Efficient and rapid radiolabeling of L5 with ^{177}Lu was achieved under mild conditions with 96% yield. The chelators exhibit near quantitative labeling efficiencies with a wide range of radio-metal ions, which are promising for the development of targeting specific radiopharmaceutical and molecular magnetic resonance imaging contrast agents.

Introduction

Macrocyclic DOTA (1,4,7,10-tetraazacyclododecane-N,N',N",N'"-tetraacetic acid) is one of the most widely used metal chelators applied for diagnostic and therapeutic applications.[1-3] It has been shown to form very stable complexes with numerous kinds of metal ions and acts as a "gold standard" chelator for gadolinium as magnetic resonance imaging (MRI) contrast agent and a number of radiometals for positron emission tomography (PET) and single-photon emission computed tomography (SPECT) imaging.[1,4] For instance, GdDOTA and $^{68}Ga/^{177}Lu$-labeled DOTA-TATE have been approved by the U.S. Food and Drug Administration (FDA) for use in human diagnostics.[5-7] Despite robust thermodynamic stability and kinetic inertness over some acyclic complexes, the radiolabeling kinetics of DOTA has always been slow and heating is required for this process, typically under acidic conditions.[1] This is problematic when applying it to temperature-sensitive molecules, such as antibodies. Therefore, the development of new chelators that enable labeling of metal ions under mild conditions with a chemical handle for targeting specificity is essential especially for use in therapeutics and radiolabeling of antibodies.

In one of our recent publications, we introduced four chiral substituents around the macrocyclic ring of DOTA to form our chiral DOTAs, we found the pre-organized cavities of the resulting chelators are favorable for fast complexation and slow metal decomplexation.[2] The chiral GdDOTAs have shown as promising and safer MRI contrast agents, while the radiolabeling of chiral DOTAs with ^{64}Cu and ^{177}Lu was shown to be more efficient than their parent DOTA by affording labeling at even milder conditions. However, ligands for diagnostic and therapeutic applications should ideally be bifunctional chelators (BFCs) to afford specific targeting, especially for the increasing demand in personalized and precision medicine which benefits from improved sensitivity and decreased side effects. Examples of complexes with vectors such as peptides and antibodies have been reported in literature, but these designs are generally limited to the DOTA system in order to not compromise the stability, hence bounded to harsher labeling conditions.[8-11] Herein, we developed three derivatives based on the ligand (L1) which has a pre-organized cavity that can assist metal complexation.

The new chelators look at different design strategies that allow a chemical handle to be incorporated for targeting with small molecules for diagnostic specificity. These designs are shown in L3-L5 (Figure 1), ligand L3 was conjugated with a cyclic arginine-glycine-aspartic acid (RGD) peptide, which exists in many biological and pathological processes where the RGD sequence is found to have molecular interactions with integrins receptors.[12-14] Another two DO3A-like chelators (DO3A = 1,4,7,10-tetraazacyclododecane-N,N',N"-1,4,7-triacetate acid) with conjugatable functional groups are designed to be BFCs (L4 & L5). The tosyl group introduced in L3 showed interactions with Human Serum Albumin (HSA) protein without effects arising from pH changes, whereas the nonadentate chelator arm design, L5,[15] demonstrated efficient radiolabeling with ^{177}Lu. These BFCs showed near quantitative labeling efficiency with various metal ions at mild labeling conditions, demonstrating potential as radiometal chelators for use with peptides and antibodies.

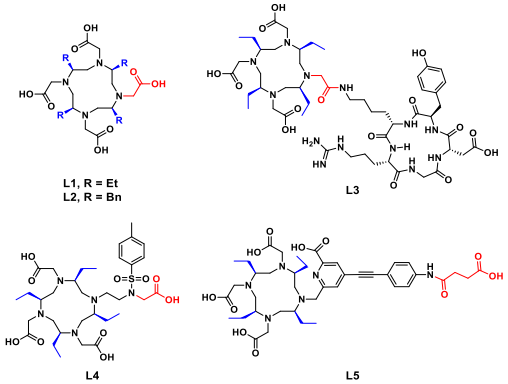

Figure 1 Structures of chelators L1 – L5 in this study.

Experimental

Materials and methods. Unless otherwise noted, all chemicals were reagent-grade and were purchased from Sigma-Aldrich or Acros Organics and used without further purification. ^{1}H and ^{13}C NMR spectra were recorded on a Bruker Ultrashield 400 Plus NMR spectrometer (at 400 MHz and 100 MHz, respectively). Chemical shifts δ were expressed in parts per million (ppm) based on the residual solvent signal in D_2O (δ 4.79 ppm), chloroform-*d* (δ 7.26 ppm) and coupling constants *J* are given in Hz. High-resolution mass spectrometry was performed on an Agilent 1260 Infinity Series apparatus with Agilent 6540 UHD Accurate-Mass Q-TOF LC/MS with detection range of 100–3200, while the low-resolution mass spectrometry and LCMS was obtained on a Waters ACQUITY UPLC H-Class-QDa mass spectrometer with detection range of 50-1250. Reverse-phase semi-preparative purification was performed on the Waters HPLC system with UV detection from 220 to 350 nm using a Waters T3 Column (250 × 19 mm). The analytical UPLC was performed on the Waters UPLC system with UV detection from 220 to 350 nm with XBridge Shield RP 18, 2.5 µm, 2.1×50 mm column. Two methods were used: Method A: mobile phase A was water with 0.05% to 0.1% TFA, mobile phase B was acetonitrile. Method B: the mobile phase A was water with 10 mM ammonium formate; mobile phase B was 90% acetonitrile/10% 10 mM ammonium formate in water. Gradient: starting from 90% A/10% B, the fraction of B increased to 90% over 8 mins, then re-equilibrated at 10% B for 4 min, the flow rate was 8 mL/min for semi-preparative HPLC; and fraction of B increased to 60% within 8 mins and then back to 10% with a flow rate of 0.2 mL/min for analytical UPLC.

UV-Vis absorption spectra of complexes were measured with an HP UV–8453 spectrophotometer (Santa Clara, CA, USA). Steady-state room temperature photoluminescence measurements were performed with an Edinburgh Instrument (Livingston, UK) FLSP920 spectrophotometer equipped with a Xe900 continuous xenon lamp, mF920 microsecond flash lamp and a single photon counting photomultiplier tube. Spectra were corrected with the bundled F900 software. Solution-state measurements were conducted using Type 23 quartz cuvettes with 10 mm path length from Starna Scientific (London, UK). Emission spectra were recorded in the range of 380-750 nm with 1 nm spectral intervals and 0.3 s integration time. Lifetime measurements were recorded base on the highest intensity emission peak of each complex and were done in triplicates. All lifetime plots were monoexponential decay.

Inductively coupled plasma - optical emission spectrometry (ICP-OES) was performed on an Agilent 700 Series system (USA), with 7 points standards (0.5 – 30 ppm) of Gd in 2% of HNO_3 for the determination of Gd metal content.

Syntheses. All the compounds were fully characterized. Experimental details and characterizations are given in Supplementary Information (NMR spectra, high-resolution ESI-MS of complexes and HPLC traces are shown in the SI).

Photophysical studies. To perform the batch titrations between lanthanide complexes (TbL4, EuL5) and the diethylenetriaminepentaacetic acid (DTPA), stock solutions of TbL4, EuL5 and DTPA were prepared in 0.1 M HEPES buffer with pH 7.3.[16] The complex solutions were diluted to identical volumes in five different vessels, then DTPA solution was added to each vessel with various complex to DTPA ratio ranged from 1:0 to 1:100. The resulting solutions were placed on a shaker at room temperature for better mixing and to equilibrate. The luminescence intensities of TbL4 and EuL5 with different concentrations of DTPA were monitored by a spectrophotometer after 24 h and up to 7 days.

HSA protein titration was conducted with TbL4 in 0.1 M HEPES buffer with pH 7.3. Lyophilized HSA (10 mg, 0.67 % w/v) was directly added to the solution of TbL4 until fully saturated and the changes in luminescence intensity were recorded.

***T*$_1$ Relaxivity measurements.** Relaxivity measurements were performed on a Bruker mq60 Minispec (Germany) with 1.4 T at 37°C. Longitudinal (T_1) relaxation times were measured using an inversion recovery experiment with 10 inversion times of duration ranging between $0.05 \times T_1$ and $5 \times T_1$. T_1 Relaxivity (r_1) was determined from the slope of a plot of $1/T_1$ vs [GdL] at 5 different concentrations. HSA binding tests were performed by adding 4.5% w/v lyophilized HSA to different concentrations of Gd^{3+} complex solutions and incubated for 30 mins at 37°C, followed by T_1 measurements. The stability test for Gd^{3+} complexes were conducted at four different conditions, which were under 0.1 M HCl, 1 M HCl, 1 equivalent of Zn^{2+} ion and 10 equivalents of Zn^{2+} ion, respectively.[2,17]

X-ray crystallographic determination. The crystal data reported in the manuscript were collected on a Bruker D8-Venture Diffractometer System with a micro-focus Mo-K α radiation. The data were collected at room temperature. Multi-scan absorption correction was applied by SADABS program,[18] and the SAINT program utilized for the integration of the diffraction profiles.[19] The structures were solved by direct method and were refined by a full-matrix least-squares treatment on F^2 using the SHELXLE program system.[20] The crystallographic data for the structural analyses have been deposited on the Cambridge Crystallographic Data Centre, CCDC No. 1901065, and the data can be obtained free of charge via www.ccdc.cam.ac.uk/data_request/cif.

Results and discussion

Syntheses of ligands and complexation studies. The ligand L3 was synthesized from the lithium salt of 2S,5S,8S,11S-2,5,8,11-tetraethyl-1,4,7,10-tetraazacyclododecane-1,4,7,10-tetraacetic acid (L1).[2] One side of the carboxylates was first activated with sulfo-NHS and EDCI at room temperature (Scheme 1), then the water solution of peptide c(RGDyK) was added. The mixture was reacted at room temperature for 2 h and purified by semi-preparative HPLC to obtain the ligand L3.

L4 was synthesized from the starting material 2S,5S,8S,11S-2,5,8,11-tetraethyl-1,4,7,10-tetraazacyclododecane (compound 1) (Scheme 2) and reacted with tosylaziridine in acetonitrile at 60°C overnight to get the compound 2. This was then reacted with tert-butyl 2-bromoacetate in the presence of potassium carbonate in acetonitrile for 16 h, resulting in compound 3. TFA deprotection resulted in ligand L4.

In L5 synthesis, the chromophore, methyl 4-((4-(4-methoxy-4-oxobutanamido)phenyl)ethynyl)-6-(((methylsulfonyl)oxy)methyl) picolinate was first dissolved in DMSO and was added dropwise into the solution mixture of the compound 1 and $NaHCO_3$ in acetonitrile at 50°C over a period of 5 h. After reacting for a further 8 h, methyl 4-((4-(4-methoxy-4-oxobutanamido)phenyl)ethynyl)-6-(((2S,5S,8S,11S)-2,5,8,11-tetraethyl-1,4,7,10-tetraazacyclododecan-1-yl)methyl)-picolinate (compound 4) was purified by semi-preparative HPLC. The purified product was then reacted with K_2CO_3 and ethyl 2-bromoacetate in acetonitrile at 50°C for 16 h, followed by the deprotection with LiOH to form L5 (Scheme 3).[15]

After successfully obtaining the ligands L3, L4 and L5, the complexation properties were tested with metal to ligand ratio in 1.05 and 2.00 in 0.1 M Tris buffer (pH 7.01). The Gd^{3+}, Eu^{3+} and Tb^{3+} solutions were prepared from lanthanide chloride hexahydrate salts and added to the aqueous solution of L3/L4/L5 with metal to ligand ratio around 1:10, the pH was adjusted to 7.0 by adding 0.1 M NaOH solution. The reaction mixtures were refluxed for 2 hours and purified by semi-preparative HPLC to obtain the pure complexes.

For metals typically used in diagnostic radiolabeling, their complexation conditions were further explored and optimised (Table 1). Similar to its parent chiral DOTA ligands, L1 and the

Scheme1 Synthesis of ligand L3

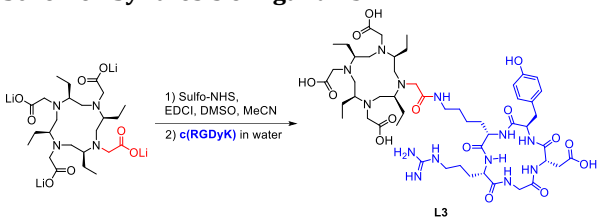

Scheme 2 Synthesis of ligand L4

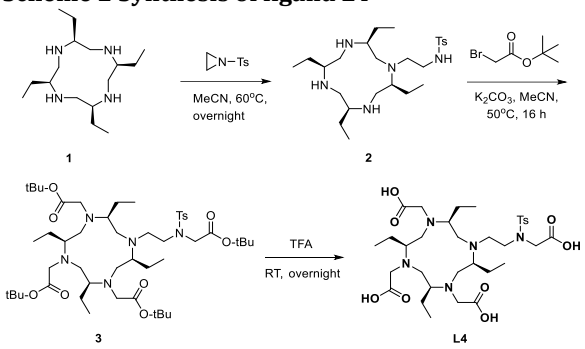

Scheme 3 Synthesis of ligand L5

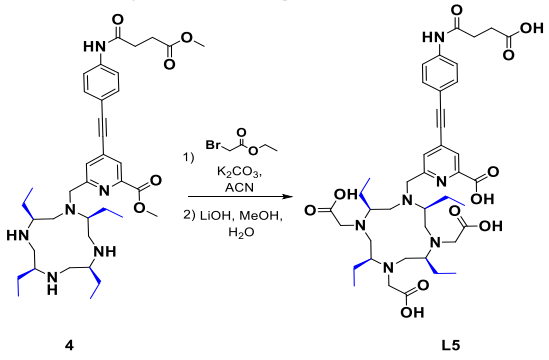

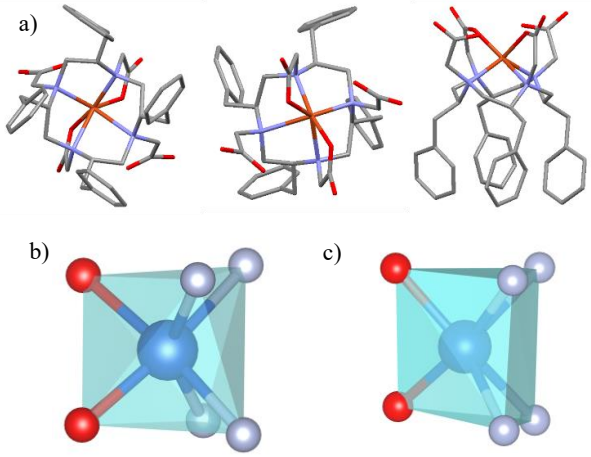

Figure 2 a) Crystal structures of CuL2 (O, red; C, grey; N, purple; Cu, orange, Hydrogen atoms are omitted for clearance). View from top (left), bottom (center) and side (right). b) Polyhedral representation of the coordination geometries of the central copper cation in CuDOTA; c) the same representation for CuL2.

Table 1. Complexation results of L3, L4 and L5 in 0.1 M Tris buffer, pH 7.01.

	Cu^{2+}				Y^{3+}				Lu^{3+}				In^{3+}				Sc^{3+}			
M/L3 ratio	M = 1.05 (2.00)				M = 1.05 (2.00)				M = 1.05 (2.00)				M = 1.05 (2.00)				M = 1.05 (2.00)			
Temp. (°C)	60		80		60		80		60		80		60		80		60		80	
Time (min)	3	60	3	60	3	60	3	60	3	60	3	60	3	60	3	60	3	60	3	60
Yield (%)	90.5 (96.4)	100	100	100	93.1 (93.6)	94.9 (100)	82.7 (91.9)	83.6 (96.6)	94.0 (94.4)	97.0 (97.9)	87.9 (96.7)	96.7	0.0 (0.0)	10.2 (10.3)	28.5 (57.7)	93.6 (98.9)	61.5	80.9	65.4 (92.7)	96.3 (98.6)
M/L4 ratio	M = 1.05 (2.00)				M = 1.05 (2.00)				M = 1.05 (2.00)				M = 1.05 (2.00)				M = 1.05 (2.00)			
Temp. (°C)	40		60		40		60		40		60		40		60		40		60	
Time (min)	3	60	3	60	3	60	3	60	3	60	3	60	3	60	3	60	3	60	3	60
Yield (%)	100	100	100	100	56.7 (69.5)	89.4 (100)	94.2 (100)	100	100	100	100	100	0.0 (0.0)	29.2 (30.1)	23.0	73.9 (80.1)	60.7	90.2 (92.7)	64.3 (94.0)	100
M/L5 ratio	M = 1.05 (2.00)				M = 1.05 (2.00)				M = 1.05 (2.00)				M = 1.05 (2.00)				M = 1.05 (2.00)			

Temp. (°C)	40		60		40		60		40		60		40		60		40		60	
Time (min)	3	60	3	60	3	60	3	60	3	60	3	60	3	60	3	60	3	60	3	60
Yield (%)	89.4 (94.2)	90.8 (94.7)	90.3 (95.1)	93.3 (95.8)	97.5	98.9	98.4 (98.8)	97.5 (99.4)	97.1 (100)	97.0	98.4	98.5	18.0 (37.0)	89.0 (97.0)	40.0 (63.5)	92.0 (95.2)	67.9 (94.2)	98.9 (99.0)	89.3 (99.5)	98.5 (99.5)

Optimal ratio of M/L, where the yield obtained at M = 2.00 is represented with ( ).

DOTA-TATE, with a cyclic peptide on one of the pendant arms, L3 also required a relatively high complexation temperature. The complexations of L3 with Lu^{3+}, Y^{3+}, Sc^{3+} and Cu^{2+} resulted in very high (~100%) complexation yields, either under 80°C for 1 h (Table 1) or 100°C for 3 mins (Table S3).[2, 21] L4 formed complexes under milder conditions (≤ 60°C) with Lu^{3+}, Y^{3+}, Sc^{3+} and Cu^{2+} with yields over 92.7%. For In^{3+}, it was notable that longer reaction time and higher temperature were required for the complexation of L4. While L4 quantitatively formed complexes with Cu^{2+} and Lu^{3+} at 40°C within 3 min. From the chemical structure, we hypothesize that the lack of one side of the pendant arm allowed a more opened cavity in L4, while after the metal ions are sequestered, the extra carboxylate near the tosyl group could turn back to coordinate with the metal ions. This phenomenon was also found in similar chelators 3p-C-DEPA and 5p-C-NETA.[22, 23] Complexations of L5 with Lu^{3+}, Y^{3+}, Sc^{3+} and Cu^{2+} were performed according to similar procedures and achieved almost instantaneous complex formations within 3 min at 40°C , though slightly better yield of over 95.8% was achieved at ~60°C, especially for Sc^{3+}. The exception here, again is the In^{3+}, which required and benefited from a longer reaction time rather than a higher temperature, with yields of 89% at 40 °C and 92% at 60°C (Table 1 & S6-7).[15,29]

Analysis of X-ray structural data. In our attempt to elucidate the coordination geometries of our copper complexes with L1, crystallization of CuL1 was performed. Despite putting huge amount of effort to grow the crystal of the CuL1, neither the two isolated isomers nor their solution mixtures produced high-quality crystal for single X-ray diffraction. Hence, to elucidate the coordination geometry of the copper chelate, we resorted to employ L2 where the phenyl rings induce a better packing in the crystallization process. The ligand L2 was synthesized as previously described.[2] The complexation of Cu^{2+} with L2 resulted in crystal of CuL2 which was obtained in a mixture of methanol and water after slow evaporation. The coordination of CuL2 is similar to the literature reported CuDOTA (Figure 2).[24] In both complexes, the Cu-O bond lengths are observed to be similar (avg. 1.95 Å in CuL2, and 1.96 Å in CuDOTA). The same two-long-two-short pattern of Cu-N bond lengths can also be found in both complexes, albeit Cu-N bonds are longer in the CuL2 (avg. 2.434 Å and 2.229 Å vs 2.318 Å and 2.107 Å in CuDOTA). The lengthened Cu-N bonds have a knocked-on effect on the dihedral angles between opposing N-Cu-N planes (avg. 72.66° in CuL2 and 77.94° in CuDOTA), as well as their coordination geometries. This is a major difference between the two complexes, with CuDOTA resembling a distorted octahedral (Figure 2b), while CuL2 appearing closer to the trigonal prismatic (Figure 2c). With similar coordination geometries, the extra chiral substituents on CuL2 create additional steric hindrance on the opposite side of the carboxylic arms.

***q* value measurement of TbL4.** To further confirm the coordination of complexes of L4, TbL4 was synthesized and its photophysical properties were used to determine the hydration number (*q* value). EuL4 was non-emissive due to the mismatching of the triplet state and thus was not used. The maximum excitation peak of TbL4 is at 253 nm (λ_{em} = 543 nm), and upon excitation with this wavelength, characteristic trivalent terbium emission was observed (Figure 3). The *q* value of TbL4 was calculated according to the lifetimes in H_2O (1.83 ms) and D_2O (3.36 ms), which was determined to be 0.94 (calculated from Parker's equation).[25] This indicates that there is one water molecule coordinated on the first sphere of the metal ion, representing that the carboxylate on the side arm is involved in the coordination. In this versatile conjugatable design of L4, the methyl group on the tosyl group can be further replaced by a nitro group and subsequently reduced to give an amino group that can be transformed into an isocyanate group for amine coupling or a textbook diazo synthesis.

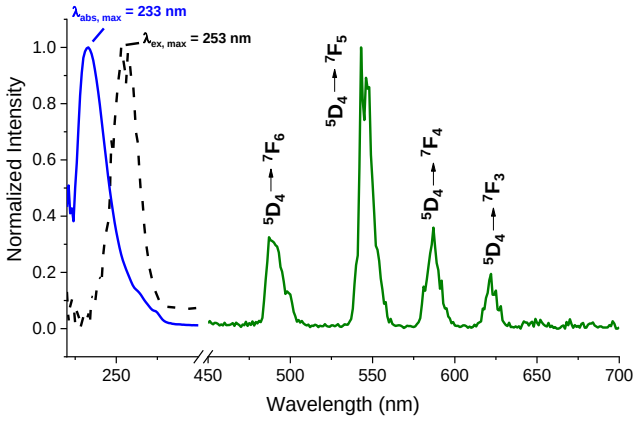

Figure 3 UV-vis absorption (blue, solid), emission (green, solid) and excitation (at 543 nm, black, dash) spectra of TbL4 at RT with pH 7.0 in water.

Competition based stability tests for TbL4 and EuL5 from Luminescent Properties. Stabilities of complexes are of immense concern in biological applications. For example, In MRI applications, gadolinium-based contrast agents (GBCAs) are commonly used. However, the decomplexation of GBCAs can lead to nephrogenic systemic fibrosis (NSF), which is associated with free Gd^{3+} ions in the body. Thus, ensuring the stabilities of metal complexes is vital in designing novel imaging and therapeutic agents. Due to the similar ionic radius of Ln^{3+}, the emissive analogs of Tb^{3+} and Eu^{3+} complexes can be used as surrogates to the Gd^{3+} complex to reflect the complex stability by competitive batch titrations with DTPA via steady state photoluminescence measurements. For this reason, competitive batch titrations with DTPA were performed with TbL4 and EuL5 (the emissive analog of our ligand series) which exhibit luminescent properties due to the presence of a suitable chromophore. L3 was not looked at, as there is no chromophore in the chleator design to afford sensitization to the Ln^{3+} ions. For TbL4 and EuL5, the luminescent intensities of both complexes were monitored up to 7 days to assess their stabilities. The effect of decomplexation will be shown by signs of a drop in luminescent intensity as neither free Tb^{3+}/ Eu^{3+} nor their complexes formed with DTPA is emissive. In the batch

titration of TbL4 (Figure 4a), there was no obvious change in the intensity during the first 3 days, and only a slight drop in the 1:50 batch on the 7th day. For EuL5 (Figure 4b), the luminescent intensity remained steady within this 7-day period. The results obtained indicated that L4 and L5 are stable for complexation in biological studies.

Relaxivity measurements and potentiometric titrations. Due to the lack of an efficient sensitizing moiety in L3, luminescence competitive batch titration cannot be conducted. Instead, T_1 relaxivity measurements were used to demonstrate the complex stability with the Gd^{3+} ion. For these studies, the Gd^{3+} complexes of all three ligands were studied and compared to DOTAREM (GdDOTA) as a benchmark. Upon monitoring GdL3-5 in 0.1 N or 1 N HCl, no obvious change in the relaxivities of GdL3-4 were noted (Figure 5 & S65) and only a slight decrease was shown for GdL5 (evident after ~20 h), showing improved stabilities compared to the GdDOTA. In the presence of physiological competing cation like Zn^{2+}, GdL3-5 all showed comparable stabilities to that of GdDOTA. (Figure S66-67)

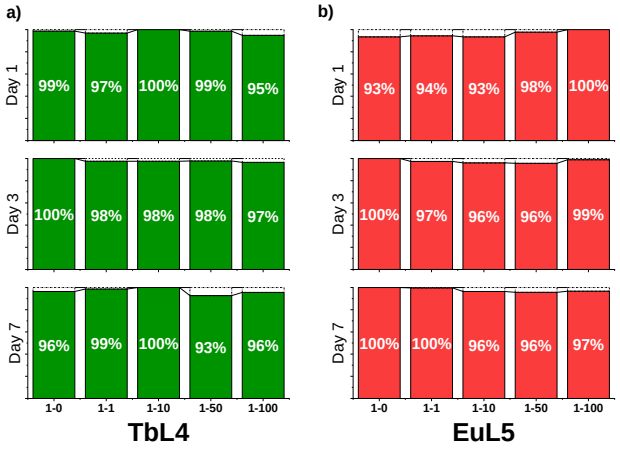

Figure 4. Relative emission intensity of a) TbL4 with different concentrations of DTPA in the batch titrations, λ_{ex} at 255 nm, from 380-750 nm within 7 days; b) EuL5 with different concentrations of DTPA in the batch titrations, λ_{ex} at 350 nm, from 380-750 nm within 7 days.

Table 2. Protonation Constants of L4, L5, DOTA and DO3A-B (I = 1.0 M KCl, 25°C)

$\log K_i^H$	L4	L5	DOTA[26]	DO3A-B[27]
$\log K_1$	10.48±0.35	10.64±0.34	11.14	11.27
$\log K_2^H$	10.14±0.30	6.50±0.03	9.69	9.19
$\log K_3^H$	8.74±0.09	4.49±0.12	4.85	4.09
$\log K_4^H$	5.10±0.03	3.40±0.08	3.95	3.07
$\sum \log K_i^H$	34.86	25.03	29.62	27.62

To further assess the stabilities of our chiral macrocycles, we also examined their protonation constants (Table 2). The protonation constants of L3 was not conducted due to numerous hydrogen-containing functional groups in the RGD peptide. The protonation constants of L4 and L5 were determined by potentiometric titration, along with DOTA and DO3A-B for comparative purposes. From the observed results, it indicated that the protonation constants of L4 are higher than for the achiral DOTA and DO3A-B ligand, whilst for L5, they are relatively similar. The similar protonation constant to the DOTA ligand is our benchmark and guideline to elucidate the stability of the complexes with DOTA complexes.[27]

From the prior work with the achiral version of L3 and also shown by the hydration number of TbL4,[8] we infer that both GdL3 and GdL4 have one water molecule coordinated to the metal ion. The inner sphere water molecule on the Gd^{3+} ions would induce the fast relaxation of the solution, making these chelators suitable as the MRI contrast agents. Hence we further examined the T_1 relaxivities of GdL3 and GdL4 (Table 3) in water and in 4.5% w/v HSA which were found to be very close to the literature values of the two isomers of GdL1.[2] This also validates their similar coordination environment.

Table 3 Summary of relaxivity ($mM^{-1}s^{-1}$) of GdL3, GdL4 and GdDOTA in water and 4.5% w/v HSA at 37° C, 1.4 T (60 MHz). [a]

Complex	Water (pH 6.5)	4.5% w/v HSA
GdL3	4.3	5.0
GdL4	4.2 (4.6)[b]	9.6 (9.7)[b]
GdDOTA[c]	3.2	4.1

a: GdL5 is fully coordinated with no water coordination, hence the value is not included in the table; b: Measured in 0.1 M citrate buffer (pH 3.0); c: Data from ref. 2.

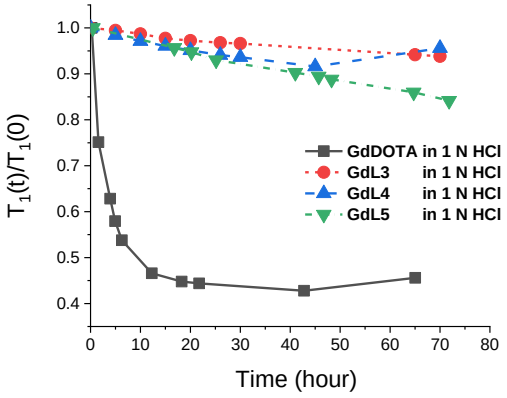

Figure 5. Evolution of T_1 relaxation time, $T_1(t)/T_1(0)$, as a function of time for GdDOTA, GdL3-5 under 1 N HCl at 37°C, 1.4T.

Here, the slightly higher relaxivity of GdL3 (M.W. = 1272.5217) arises from the relatively higher molecular weight due to the attached RGD peptide. Comparing to GdL3, GdL4 have a similar relaxivity in water, but a much higher relaxivity in HSA solution. This is observed due to the aromatic nature of the tosyl group, which binds with the HSA protein, hence the prolonged rotational correlation time of the bound complex induced the enhanced relaxivity. The binding is also supported by the photoluminescence measurements of TbL4, which in the presence of HSA gives a turn-off phenomenon in the emission spectrum (Figure 6). It should be noted that the relaxivities of some similar complexes with tosyl groups are pH-sensitive.[28] The proton on the sulfamide, however, is substituted in our complex of GdL4, so the pH-sensitively parameter is eliminated and is not apparent in our complex.

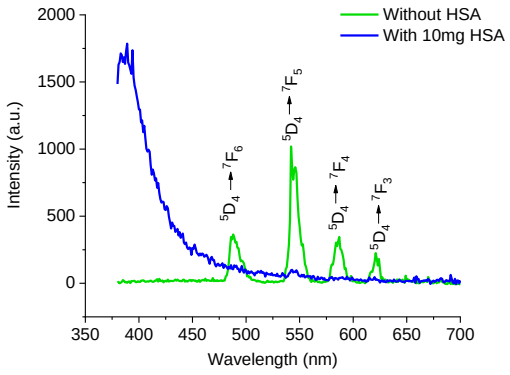

Figure 6 Emission spectra of TbL4 without adding HSA (green) and with 10 mg HSA added (blue) in 0.1 M HEPES, pH 7.3, excited at 255 nm.

Radiolabeling. In order to show the versatility of our BFCs and their potential for therapeutics, we further studied the radiolabeling with selected radiometals that are suitable for PET with our BFCs. From the complexation results, although L3 and L4 were rather suitable for ^{64}Cu labeling, L3 was selected for further radiolabeling studies as it is conjugated with a RGD peptide and can be used to investigate the robustness of peptides in radiolabeling conditions.

Similar to the complexation with Cu^{2+}, L3 was successfully radiolabeled with $^{64}Cu^{2+}$ in 0.5 M NH_4OAc buffer (pH 6.05) after heating at 40°C for 30 min. The radiolabeling yield was >99% with negligible free $^{64}Cu^{2+}$ remaining (Figure S58).

We then examined the nonadentate chelator L5 to test out the radiolabeling efficiency with $^{177}Lu^{3+}$. Nonadentate chelators are generally more suitable for f-block elements as a saturated coordination sphere improves the stabilities of the complexes formed while assisting in the chelating efficiency as well. This had also been shown in our previous studies of compounds with a chiral DO3A backbone and a bidentate chromophore.[29,30] In our radiolabeling studies, L5 gave a very effective radiolabeling with $^{177}Lu^{3+}$, with 96% yield obtained after reacting at 45°C within 15 mins (pH 6.0) (Figure S59). This labeling efficiency was still maintained when the pH was increased to the physiological pH 7.0 (94% yield, at 45°C, 15 mins) (Figure S60). Such mild reaction conditions enable L5 to be a potential chelator for radiolabeling of sensitive biomolecules, such as antibodies and peptides. We believe the design of L5 as a radiometal chelator will provide a new strategy for using nonadentate macrocyclic chelator for radiopharmaceutical applications.

Conclusions

In conclusion, we showed that by strategic design, tailored chelators based on our chiral cyclen designs can give rise to a series of ligands that are versatile for different metals. Our chiral DOTAs and their derivatives possess significant potential as radiolabeling chelators for PET/SPECT, as well as in the development of improved diagnostic agents such as for MRI and radioimmunoassay applications. Further biological studies of these compounds are on going in our laboratory to further maximize the potential for use in theranostics and imaging.

ASSOCIATED CONTENT

Supporting Information

Experimental procedures, full characterization of products, HPLC traces, NMR spectra, and graphs of lifetime measurements. This material is available free of charge via the Internet at http://pubs.acs.org

Accession Codes

CCDC 1901065 contains the supplementary crystallographic data for this paper.

AUTHOR INFORMATION

Corresponding Author

*** ga-lai.law@polyu.edu.hk**

Present Addresses

X. L currently at Regeneron Pharmaceuticals, Inc.

Author Contributions

G.-L. L. conceived and supervised the project. All authors have given approval to the final version of the manuscript. ‡These authors contributed equally.

ACKNOWLEDGMENT

Funding Sources

G.-L. L and J. Z gratefully acknowledge the Research Grants Council of Hong Kong (PolyU153009/19P and PolyU153013/17P), the State Key Laboratory of Chemical Biology and Drug Discovery, the Hong Kong Polytechnic University ((a) University Research Facility in Chemical and Environmental Analysis (UCEA); (b) University Research Facility in Life Sciences (ULS))

C.J.A and X. L acknowledge funding from the Department of Medicine at the University of Pittsburgh.

Notes

The authors declare no competing financial interests.

ABBREVIATIONS

Cyclen, 1,4,7,10-Tetraazacyclododecane; DOTA, 1,4,7,10-tetraazacyclododecane-N,N',N",N'"-tetraacetic acid; DO3A , 1,4,7,10-tetraazacyclododecane-N,N',N"-1,4,7-triacetate acid.

References

(1) Kostelnik, T. I.; Orvig, C. Radioactive Main Group and Rare Earth Metals for Imaging and Therapy. *Chem. Rev.* **2019,** *119* (2), 902.

(2) Dai, L.; Jones, C. M.; Chan, W. T. K.; Pham, T. A.; Ling, X.; Gale, E. M.; Rotile, N. J.; Tai, W. C.-S.; Anderson, C. J.; Caravan, P.; Law, G.-L. Chiral DOTA chelators as an improved platform for biomedical imaging and therapy applications. *Nat. Commun.* **2018,** *9* (1), 857.

(3) Stasiuk, G. J.; Long, N. J. The ubiquitous DOTA and its derivatives: the impact of 1, 4, 7, 10-tetraazacyclododecane-1, 4, 7, 10-tetraacetic acid on biomedical imaging. *Chem. Commun.* **2013,** *49* (27), 2732.

(4) Wahsner, J.; Gale, E. M.; Rodriguez-Rodriguez, A.; Caravan, P. Chemistry of MRI Contrast Agents: Current Challenges and New Frontiers. *Chem. Rev.* **2019,** *119* (2), 957.

(5) Pierre, V. C.; Allen, M. J.; Caravan, P. Contrast agents for MRI: 30+ years and where are we going? *J. Biol. Inorg. Chem.* **2014,** *19* (2), 127.

(6) FDA approves 18F-fluciclovine and 68Ga-DOTATATE products. *J. Nucl. Med.* **2016**, *57*(8), 9N.

(7) FDA approves Lutathera for GEP NET therapy. *J. Nucl. Med*. **2018**, *59*(4), 9N.

(8) Autio, A.; Henttinen, T.; Sipila, H. J.; Jalkanen, S.; Roivainen, A., Mini-PEG spacering of VAP-1-targeting 68Ga-DOTAVAP-P1 peptide improves PET imaging of inflammation. *EJNMMI Res* **2011,** *1*, 10.

(9) Breeman, W. A.; De Jong, M.; Visser, T. J.; Erion, J. L.; Krenning, E. P. Optimising conditions for radiolabelling of DOTA-peptides with ^{90}Y, ^{111}In and ^{177}Lu at high specific activities. *Eur. J. Nucl. Med. Mol. Imaging* **2003**, 30, 917-20.

(10) Mohsin, H.; Jia, F.; Sivaguru, G.; Hudson, M. J.; Shelton, T. D.; Hoffman, T. J.; Cutler, C. S.; Ketring, A. R.; Athey, P. S.; Simón, J.; Frank, R. K.; Jurisson, S. S.; Lewis, M. R. Radiolanthanide-Labeled Monoclonal Antibody CC49 for Radioimmunotherapy of Cancer: Biological Comparison of DOTA Conjugates and 149Pm, 166Ho, and 177Lu. *Bioconjugate Chem.* **2006,** *17* (2), 485.

(11) Rasaneh, S.; Rajabi, H.; Babaei, M. H.; Johari Daha, F. Synthesis and biodistribution studiesof ^{177}Lu-trastuzumab as a therapeutic agent in the breast cancer mice model. *J. Label. Compd. Radiopharm.* **2010**, 53, 575-579.

(12) Ye, Y.; Bloch, S.; Xu, B.; Achilefu, S., Design, synthesis, and evaluation of near infrared fluorescent multimeric RGD peptides for targeting tumors. *J Med Chem* **2006,** *49* (7), 2268-75.

(13) Bellis, S. L., Advantages of RGD peptides for directing cell association with biomaterials. *Biomaterials* **2011,** *32* (18), 4205-10.

(14) Alipour, M.; Baneshi, M.; Hosseinkhani, S.; Mahmoudi, R.; Jabari Arabzadeh, A.; Akrami, M.; Mehrzad, J.; Bardania, H., Recent progress in biomedical applications of RGD-based ligand: From precise cancer theranostics to biomaterial engineering: A systematic review. J Biomed Mater Res A 2020, 108 (4), 839-850.

(15) Zhang, J.; Dai, L.; Webster, A. M.; Chan, W. T. K.; Mackenzie, L. E.; Pal, R.; Cobb, S. L.; Law, G.-L., Unusual Magnetic Field Responsive Circularly Polarized Luminescence Probes with Highly Emissive Chiral Europium(III) Complexes. *Angew. Chem. Int. Ed.* **2020**, *59*, 2-9.

(16) D'Aleo, A.; Moore, E. G.; Xu, J.; Daumann, L. J.; Raymond, K. N., Optimization of the Sensitization Process and Stability of Octadentate Eu(III) 1,2-HOPO Complexes. *Inorg Chem* **2015,** *54* (14), 6807-20.

(17) Jody L. Major, G. P., Claudio Luchinat, and Thomas J. Meade, The synthesis and in vitro testing of a zinc-activated MRI contrast agent. *PNAS* **2007,** *104* (35), 13881-13886.

(18) Krause, L., Herbst-Irmer, R., Sheldrick, G. M. & Stalke, D. J. , *Appl. Crystallogr.* **2015**, 48.

(19) Bruker-AXS. APEX3 Software Suite. Bruker, Madison, Wisconsin, USA. 2014.

(20) Hübschle, C. B. S., G. M.; Dittrich, B., ShelXle: a Qt Graphical User Interface for SHELXL. *J. Appl. Cryst.* **2**011, 44, 1281-1284.

(21) Liu, F.; Zhu, H.; Yu, J.; Han, X.; Xie, Q.; Liu, T.; Xia, C.; Li, N.; Yang, Z., (68)Ga/(177)Lu-labeled DOTA-TATE shows similar imaging and biodistribution in neuroendocrine tumor model. *Tumour Biol.* **2017**, *39* (6), 1010428317705519.

(22) Song, H. A.; Kang, C. S.; Baidoo, K. E.; Milenic, D. E.; Chen, Y.; Dai, A.; Brechbiel, M. W.; Chong, H.-S. Efficient Bifunctional Decadentate Ligand 3p-C-DEPA for Targeted α -Radioimmunotherapy Applications. *Bioconjugate Chem.* **2011,** *22* (6), 1128.

(23) Kang, C. S.; Chen, Y.; Lee, H.; Liu, D.; Sun, X.; Kweon, J.; Lewis, M. R.; Chong, H.-S. Synthesis and evaluation of a new bifunctional NETA chelate for molecular targeted radiotherapy using ^{90}Y or ^{177}Lu. *Nucl. Med. Biol.* **2015,** *42* (3), 242.

(24) Riesen, A.; Zehnder, M.; Kaden, T. A. Metal complexes of macrocyclic ligands. Part XXIII. Synthesis, properties, and structures of mononuclear complexes with 12- and 14-membered tetraazamacrocycle-N,N′,N″,N‴-tetraacetic Acids. *Helv. Chim. Acta* **1986,** *69* (8), 2067.

(25) Beeby, A.; M. Clarkson, I.; S. Dickins, R.; Faulkner, S.; Parker, D.; Royle, L.; S. de Sousa, A.; A. Gareth Williams, J.; Woods, M. Non-radiative deactivation of the excited states of europium, terbium and ytterbium complexes by proximate energy-matched OH, NH and CH oscillators: an improved luminescence method for establishing solution hydration states. *J. Chem. Soc., Perkin Trans. 2* **1999**, 493.

(26) Clarke, E. T.; Martell, A. E. Stabilities of trivalent metal ion complexes of the tetraacetate derivatives of 12-, 13- and 14-membered tetraazamacrocycles. *Inorganica Chim. Acta* **1991,** *190* (1), 37.

(27) Tóth, É.; Király, R.; Platzek, J.; Radüchel, B.; Brücher, E. Equilibrium and kinetic studies on complexes of 10-[2, 3-dihydroxy-(1-hydroxymethyl)-propyl]-1, 4, 7, 10-tetraazacyclododecane-1, 4, 7-triacetate. *Inorg. Chim. Acta* **1996,** *249* (2), 191.

(28) Lowe, M. P.; Parker, D.; Reany, O.; Aime, S.; Botta, M.; Castellano, G.; Gianolio, E.; Pagliarin, R. pH-dependent modulation of relaxivity and luminescence in macrocyclic gadolinium and europium complexes based on reversible intramolecular sulfonamide ligation. *J. Am. Chem. Soc.* **2001,** *123* (31), 7601.

(29) Dai, L.; Lo, W.-S.; Coates, I. D.; Pal, R.; Law, G.-L. New Class of Bright and Highly Stable Chiral Cyclen Europium Complexes for Circularly Polarized Luminescence Applications. *Inorg. Chem.* **2016,** *55* (17), 9065.

(30) Dai, L.; Lo, W.-S.; Zhang, J.; Law, G.-L. One-Step Reaction for Screening of Chromophores to Improve the Luminescence of Lanthanide Complexes. *Asian J. Org. Chem.* **2017,** *6* (12), 1845.

Table of contents graphics

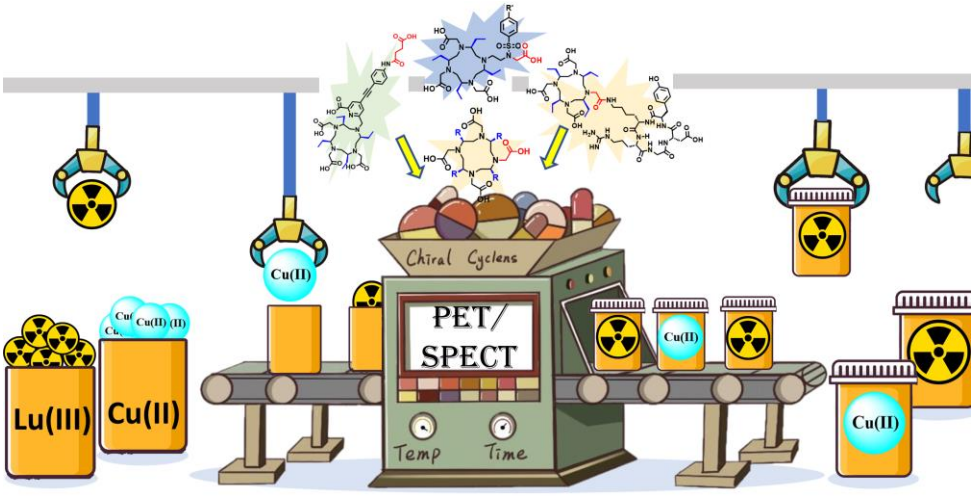

Chiral conjugatable macrocyclic ligand designs for encapsulating different radioactive metals were synthesized, which possess advantages such as rapid complexation, and ability for conjugation to targeting vectors compared to the clinical approved radiolabeled DOTA. These chiral macrocyclic ligands serve as a new platform for novel ligand design as well as shows potential to be radiometal chelator for imaging modalities such as PET and SPECT.